

FeCl₃-supported solvothermal liquefaction of *Miscanthus* in methanol

Ying Su^{a,b,*}, Bingfeng Guo^{b,c,**}, Ursel Hornung^b, Nicolaus Dahmen^b

^a Yancheng Institute of Technology, College of Civil Engineering, Yancheng, 224051, China

^b Karlsruhe Institute of Technology, Institute for Catalysis Research and Technology, Eggenstein-Leopoldshafen, Germany

^c Shanghai Key Laboratory of Atmospheric Particle Pollution and Prevention (LAP3), Department of Environmental Science and Engineering, Fudan University, Shanghai, 200438, China

ARTICLE INFO

Keywords:

Biomass valorization
Solvothermal liquefaction
Miscanthus
FeCl₃ pre-soaking
Methanol

ABSTRACT

Solvothermal liquefaction is a technique that could be used to convert biomass into value-added chemicals. Here, *Miscanthus* was soaked in FeCl₃ before solvothermal liquefaction to improve the conversion rate and prevent corrosion of the reactor. Dried *Miscanthus* (DM), *Miscanthus* pre-soaked in FeCl₃ (MSFe), and *Miscanthus* with FeCl₃ added directly (MAFe) were liquefied in methanol in an autoclave at between 150 and 350 °C. The conversion rates were higher for MSFe and MAFe than DM below 300 °C. At 225 °C, the conversion rate was higher for MSFe (45.1 wt%) than MAFe (36.1 wt%) and more furfural derivatives were produced from MSFe than MAFe. The MSFe and MAFe conversion rates were both ~70 wt% when supercritical methanol was used. The different liquid products contained similar chemicals (phenol derivatives, furfural derivatives, carbohydrate derivatives, and esters). The derivatives formed through alkylation reactions between intermediates and methanol. Under subcritical conditions, a higher conversion rate was achieved and more value-added chemical derivatives were produced from MSFe than DM or MAFe. This may mainly be because FeCl₃ assists in the cleavage of ether bonds by forming chelates with phenolic groups and because pre-soaking creates a concentration gradient in the microenvironment around *Miscanthus*.

1. Introduction

Attempts are being made to find alternatives to fossil fuels because using alternatives to fossil energy could mitigate climate change and the negative effects of emissions caused by combusting fossil fuels on human health. Biomass is currently the most commonly used type of renewable fuel. Biomass is readily obtained in most of the world [1]. *Miscanthus* is a useful crop for producing biofuels and chemicals because it contains abundant cellulose, hemicellulose, and lignin [2,3]. Attempts have been made to maximize biomass utilization and valorization, and there is increasing interest in using biomass to produce platform or value-added chemicals such as phenolic and other aromatic compounds [1,4,5] and furfurals [6]. These chemicals are usually produced through thermochemical processes. Hydrothermal liquefaction (HTL) is one of the most effective thermochemical processes for producing biofuels and biomass-based chemicals [7]. HTL is usually performed in liquid water at 250–400 °C and a high pressure (10–25 MPa) and has the clear benefit of directly liquefying wet biomass to give a biocrude product [8–10]. The key biomass valorization step is transformation of large polymers

into small molecules [11].

A catalyst is useful for improving the biomass conversion rate and increasing the product yield [12]. Iron is a very cheap and effective catalyst [13,14]. FeCl₃ is a Lewis acid catalyst that has been found to effectively improve biomass conversion with a high degree of selectivity [15]. It has been found that the presence of FeCl₃ during the HTL pretreatment process before *Miscanthus* is enzymatically hydrolyzed can promote the degradation of xylose or xylan to furfural [16,17]. Chen et al. [18] found that the effluent from FeCl₃ pretreatment before enzymatic hydrolysis of bagasse contained furfural and 5-hydroxymethylfurfural at concentrations of 5.1 and 0.8 g L⁻¹, respectively. Chen et al. [19] studied the conversion of saccharides into furfurals in the presence of FeCl₃ and found that FeCl₃ is the best catalyst for producing furfural products from precursors. FeCl₃ strongly interacts with biomass and can increase the degree of hydrolysis that occurs and the amounts of furfurals produced. In each study mentioned above, FeCl₃ was added directly to the biomass HTL reactor to pretreat the biomass. This could lead to corrosion of the reactor. Amarasekara et al. [20] pretreated switchgrass by impregnating the switchgrass with FeCl₃ and then applying heat or microwaves and found that the pretreatment improved

* Corresponding author. Yancheng Institute of Technology, College of Civil Engineering, Yancheng, 224051, China.

** Corresponding author. Karlsruhe Institute of Technology, Institute for Catalysis Research and Technology, Eggenstein-Leopoldshafen, Germany.

E-mail addresses: ying@ycit.cn (Y. Su), bingfeng.guo@kit.edu (B. Guo).

List of abbreviations

DM	Dried <i>Miscanthus</i>
MSFe	<i>Miscanthus</i> pre-soaked in FeCl ₃
MAFe	<i>Miscanthus</i> with FeCl ₃ added directly
HTL	Hydrothermal liquefaction

the total yields of reducing sugars when the biomass was subsequently hydrolyzed at 160 °C. Pre-soaking biomass is a good pretreatment for promoting the formation of reducing sugars. However, it is unclear whether pre-soaking also promotes the production of other value-added chemicals during HTL or solvothermal liquefaction. It is also not clear whether pre-soaking biomass in FeCl₃ and adding FeCl₃ directly to the reactor give different liquefaction products and different yields.

In the study described here, Chinese reeds (*Miscanthus giganteus*) pre-soaked with FeCl₃ in solvent were used as feedstock biomass in a liquefaction and valorization process. FeCl₃ was used because it is a homogeneous catalyst that readily comes into contact with the substrate molecules. Heterogeneous catalysts cannot readily be used with solid biomass. The aim of pre-soaking the biomass was to distribute the catalyst evenly through the feedstock and ensure that it is not easily washed out of the feedstock by the solvent. This should decrease the amount of corrosion of the reactor that occurs. *Miscanthus* pre-soaked with FeCl₃ in solvent could improve the ability of the catalyst to be recycled because the FeCl₃ could remain in the biomass and be regenerated during subsequent biomass processing (e.g., incineration). Solvothermal liquefaction was performed because it allows the reactants and intermediates to be dissolved as much as possible [21,22], requires milder conditions than pyrolysis [21], and gives a biocrude product with a good volumetric energy density and a low O/C ratio and acidity [23] because deoxygenation occurs during the process. Methanol was used because it is a readily available hydrogen donor that can be produced from renewable sources [4,22] and plays an important role in the production of phenolic monomers and the depolymerization of lignin [24]. Methanol also affects lignin conversion and deoxy-liquefaction [4,25]. Both the FeCl₃ catalyst and the solvent will be involved in biomass degradation, so solvothermal liquefaction of *Miscanthus* should be more efficient if the *Miscanthus* is pre-soaked in FeCl₃.

This study is innovative because addition of FeCl₃ and liquefaction were performed as two separate steps (i.e., the biomass was impregnated with FeCl₃ and then subjected to the liquefaction process) to minimize corrosion of the HTL reactor and facilitate recovery of the FeCl₃. The different effects of pre-soaking the biomass in FeCl₃ and adding FeCl₃ directly to the reactor were assessed. Dried *Miscanthus* (DM), *Miscanthus* pre-soaked in FeCl₃ (MSFe), and *Miscanthus* with FeCl₃ added directly (MAFe) were liquefied in subcritical or supercritical methanol and the results for the different *Miscanthus* substrates were compared. The aim was to develop a strategy for converting biomass into value-added chemicals. The *Miscanthus* conversion process and the product yields were assessed. The chemical compositions of the biocrude products were identified and determined by gas chromatography (GC) mass spectrometry (MS), the molecular structures of the biocrude products were investigated by nuclear magnetic resonance spectroscopy, the molecular sizes of the biocrude products were determined by gel permeation chromatography, and the properties of the solid products were investigated by thermogravimetric analysis (TGA), Fourier-transform infrared (FTIR) spectroscopy, and X-ray diffractometry.

2. Materials and methods

2.1. Materials

Miscanthus biomass was obtained from the University of Hohenheim

in July 2019. The properties of *Miscanthus* are shown in Table 1. The biochemical composition and metal (except Fe) contents were determined by staff at the University of Hohenheim, and the other properties were determined before the *Miscanthus* was used. The *Miscanthus* biomass was dried at 105 °C before use. FeCl₃ was purchased from Sigma-Aldrich. Technical methanol was used as the solvent. The autoclave had a volume of 25 mL and was made of EN 1.4571 stainless steel.

2.2. Solvothermal liquefaction and separation of the products

A 1.0 g aliquot of *Miscanthus* with 10 wt% catalyst and 10.0 mL methanol were added to the autoclave, then N₂ was fed into the autoclave at a pressure of 5.0 × 10⁴ Pa to remove the residual air. The *Miscanthus* biomass was soaked in FeCl₃ in solvent for 2 h before use for most of the experiments.

The autoclave was heated in a sand bath. Reaction temperatures between 150 and 350 °C were used, and the reaction time was 35 min (5 min to reach the reaction temperature and 30 min for the reaction). At the end of the reaction time, the autoclave was cooled with water and then the products were separated and analyzed. The liquefaction and separation processes are shown in Fig. 1.

The autoclave was weighed after the reaction (to give mass M₁) and after being opened (to give mass M₂). The gaseous product mass W_G was defined as W_G = M₁ - M₂ - M_{N₂}, where M_{N₂} is the mass of N₂ in the autoclave. The solid-liquid mixture was then passed, under vacuum, through a Whatman nylon 0.45 μm membrane filter. The filtrate was collected and weighed (to give mass L₁). The wet solid residue was weighed, dried at 105 °C and then weighed again (to give mass W_S), and the decrease in mass caused by drying was defined as the mass of the liquid products retained by the solid (L₂). The total mass of liquid products W_L was defined as W_L = L₁ + L₂. The *Miscanthus* conversion rate was calculated from the amount of dry *Miscanthus* added to the autoclave using Equation (1). The product yields were calculated using Equations (2)–(4).

$$\text{Conversion (wt\%)} = 100 \cdot \frac{W_S}{W_M} \cdot 100 \quad (1)$$

$$\text{Gaseous products yield (wt\%)} = \frac{W_G}{W_T} \cdot 100 \quad (2)$$

$$\text{Liquid products yield (wt\%)} = \frac{W_L}{W_T} \cdot 100 \quad (3)$$

$$\text{Solid products yield (wt\%)} = \frac{W_S}{W_T} \cdot 100 \quad (4)$$

In Eqs. (1)–(4), W_T, W_M, W_G, W_S, and W_L are the masses of total feedstock (*Miscanthus*, methanol, and FeCl₃), *Miscanthus*, gaseous products, solid products, and liquid products, respectively. Each liquefaction experiment was performed twice or more.

2.3. Product analysis

The gaseous product composition was determined by GC using an Agilent 6890 N instrument (Agilent Technologies, USA) with thermal conductivity and flame-ionization detectors. The molecular weight (M_w) distribution of each liquid sample was determined by gel permeation chromatography using a Merck Hitachi DAD L-2455 instrument fitted an A2500 aqueous column (30 cm long, 8 mm i. d.; Malvern Panalytical, UK) and a Hitachi L-2490 RI detector (Hitachi High-Technologies, Japan) and using dimethyl sulfoxide as the eluent. The compounds in each liquid product were identified by GC-MS using an Agilent 6890 N instrument (Agilent Technologies) equipped with an Agilent 5973 network mass selective detector (Agilent Technologies). The oven temperature program started at 70 °C, which was held for 2 min, then increased at 8 °C min⁻¹ to 180 °C, and then increased at 4 °C min⁻¹ to

Table 1
Properties of *Miscanthus*.

Moisture content (wt%)	Ash (wt%)	Elemental analysis (wt%)					HHV ^b (MJ kg ⁻¹)
		C	H	N	S	O ^a	
9.15	1.96	45.5	6.3	0.2	0.1	45.9	18.03
Biochemical composition (wt%)		Metal content (wt%)					
Cellulose	Hemicellulose	Lignin	K	P	Ca	Mg	Fe
51.86	17.55	14.04	0.66	0.02	0.05	0.01	0.07

^a By difference (O% = 100% ash% C% N% S% H%).

^b HHV (MJ/kg) = (0.3516 × C) + (1.16225 × H) - (0.1109 × O) + (0.0628 × N) + (0.10465 × S)

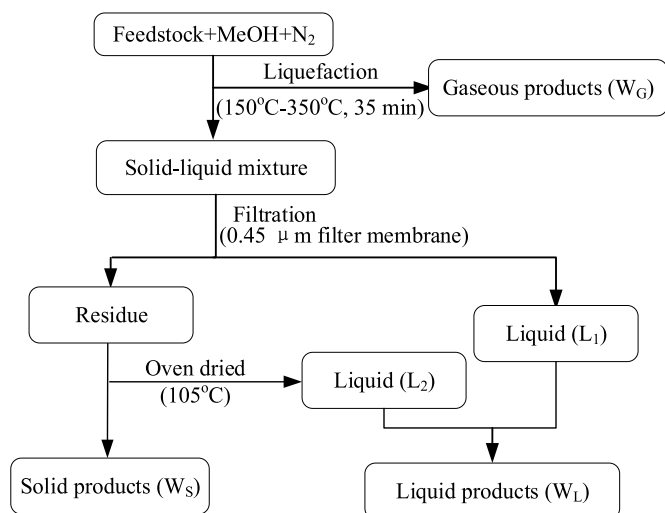


Fig. 1. Liquefaction and separation processes.

280 °C, which was held for 10 min. Separation was achieved using an RTX-5MS column (0.25 mm i. d., 0.25 μm film thickness; Restek, USA). The carrier gas was helium, and the flow rate was 1.5 mL min⁻¹. Heteronuclear single quantum coherence (HSQC) spectra of the liquid products were acquired using a 2D-nuclear magnetic resonance spectroscopy instrument. The functional groups were identified using MestReNova software 10. The Fe content of each liquid product was determined using an Agilent 725 inductively coupled plasma optical emission spectrometer (Agilent Technologies).

Samples were subjected to TGA using a Mettler Toledo 2LF instrument (Mettler-Toledo, Greifensee, Switzerland) using a flowing N₂ atmosphere (flow rate 50 mL min⁻¹). A sample was heated from 25 to 800 °C at a heating rate of 10 °C min⁻¹. FTIR spectra of the solid products were acquired using a Varian 660-IR spectrometer (Shimadzu, Japan). A sample was mixed with KBr and pressed into a disk for analysis over the wavelength range 400–4000 cm⁻¹. Eight replicate scans were performed for each sample, and the average of the spectra was used. X-ray powder diffractometry patterns of the solid products were acquired using a PANalytical X'Pert Pro X-ray diffractometer (Malvern Panalytical) using Bragg–Brentano geometry, Cu Kα radiation, and a Ni filter. For each sample, the 2θ range 5°–120° was analyzed in 1 h.

3. Results

3.1. Effects of different reaction conditions on *Miscanthus* conversion

The product yields and *Miscanthus* conversion rates found at different reaction temperatures are shown in Fig. 2. As shown in Fig. 2(a), most of the products were recovered, and between 12.1 wt% and 30.1 wt% of the mass was lost. The masses of the gaseous products when MSFe and MAFe were reacted at 350 °C were 2.843 and 2.661 g, respectively. The gaseous product masses were higher than the mass of feedstock that was used (1.0 g). The gaseous products must therefore have formed from both the solid and solvent, indicating that methanol was a reactant. The main non-condensable gaseous products of MSFe were CO₂, CH₄, CO, and H₂, which contributed (ignoring other gases and considering the total volume of these four gases to be 100%) 83.1 vol%, 1.4 vol%, 15.5 vol%, and 0.0 vol%, respectively, of the non-condensable gaseous products when the reaction temperature was 250 °C and 44.2 vol%, 26.1 vol%, 18.0 vol%, and 11.6 vol%, respectively, of the non-

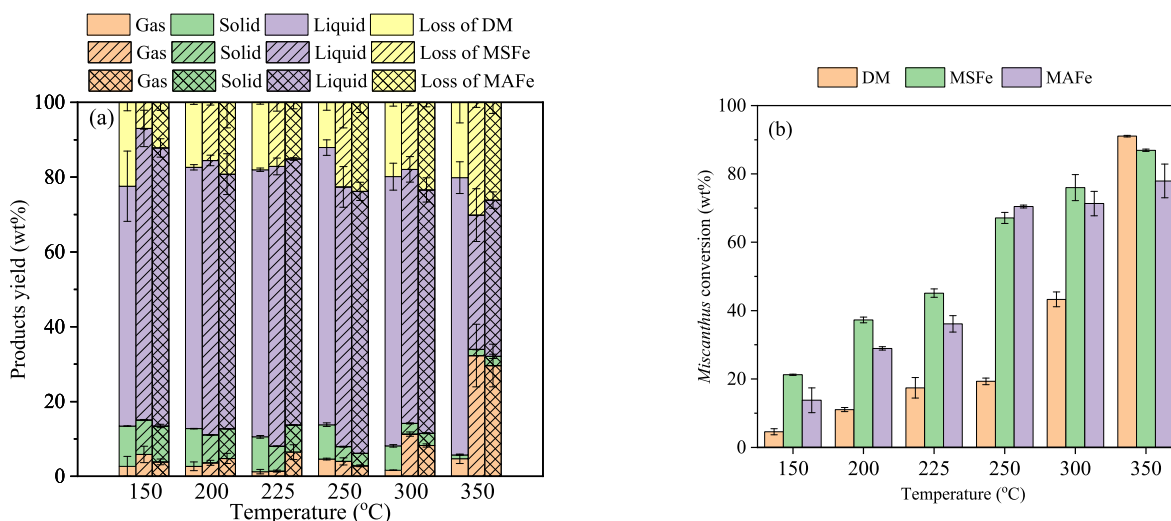


Fig. 2. (a) Product distributions and (b) *Miscanthus* conversion rates found at different reaction temperatures.

condensable gaseous products when the reaction temperature was 350 °C. The dramatic increase in the contribution of CH₄ to the total volume as the reaction temperature increased indicated that more demethylation occurred as the reaction temperature increased.

The *Miscanthus* conversion rates found when DM, MSFe, and MAFe were treated at different reaction temperatures are shown in Fig. 2(b). The conversion rates for DM, MSFe, and MAFe (i.e., without or with FeCl₃ present) increased as the reaction temperature increased up to 350 °C. At ≤300 °C, the conversion rates were much higher for MSFe and MAFe than DM. At 225 °C, the conversion rate was higher for MSFe (45.1%) than MAFe (36.1%). However, at 250 °C, the conversion rates for MSFe and MAFe were very similar, 67.1% and 70.4%, respectively. Zeng et al. [26] found a conversion yield of 66% for hardwood lignin liquefied using supercritical ethanol. Higher conversion rates might be achieved using methanol above the critical point (512.6 K (239.5 °C) at 8.09 MPa) than using subcritical methanol [27]. Increasing the temperature will cause the feedstock to mix more evenly with supercritical methanol, and this would have decreased the difference between the results achieved using MSFe and MAFe. At 350 °C, the conversions rates were lower for MSFe and MAFe than DM. There are two possible reasons for this. FeCl₃ could have increased the degree of re-polymerization that occurred, which would have caused more solid products to form. This would be consistent with the conclusion drawn by Perera et al., that under supercritical conditions increasing the temperature increases the solid and gaseous product yields and decreases the bio-oil yield because of re-polymerization of intermediate products at high temperatures [28]. Alternatively, Fe³⁺ could form Fe₃O₄ at 350 °C and enter the solid products (see section 3.3.3).

3.2. Characterization of the liquid products

The conversion rates achieved under different reaction conditions were determined and the FeCl₃ pre-soaking content and pre-soaking time were optimized. It can be seen from Fig. 2(b) that the maximum conversion rate was found at 250 °C with FeCl₃ present. Therefore, the conversion rates were determined using different FeCl₃ pre-soaking contents and a reaction temperature of 250 °C. The results are shown in Fig. 3(a). Increasing the FeCl₃ pre-soaking content affected the product distribution little but increased the *Miscanthus* conversion rate. The conversion rate was 68.3% when *Miscanthus* was pre-soaked in 10 wt% FeCl₃ and 75.5% when *Miscanthus* was pre-soaked in 15 wt% FeCl₃. The optimum FeCl₃ pre-soaking content from an economic point of view was 10 wt%. It can be seen from Fig. 3(b) that conversion rates of 65.7%–70.4% were found when MSFe was used with different pre-soaking times. This indicated that the pre-soaking time affected the *Miscanthus* conversion rate little. This indicated that the FeCl₃ reacted

with *Miscanthus* effectively and quickly.

3.2.1. M_w distributions of the liquid products

The M_w distributions of the liquid products of the reactions performed at 225 and 250 °C are shown in Fig. 4. The liquid product molecules were divided into groups according to their M_ws determined by gel permeation chromatography. The numbers next to the columns in Fig. 4 are the mean M_ws of the different groups.

The liquid products of MSFe and MAFe reacted at 225 °C had similar M_w distributions. The MSFe and MAFe products both had four M_w groups, but the DM products had five M_w groups. This indicated that *Miscanthus* degradation was promoted by FeCl₃. As shown in Fig. 5(b), the products of MSFe and MAFe had lower molecular ranges when the reaction temperature was 250 °C than when the reaction temperature was 225 °C. A MSFe and MAFe product molecule group with a mean M_w of ~2600 was found when the reaction temperature was 225 °C but was not found (i.e., the products had decomposed) when the reaction temperature was 250 °C. The MSFe and MAFe product molecules with M_ws of 4042–4030 found when the reaction temperature was 225 °C had M_ws of 3848–3829 when the reaction temperature was 250 °C, indicating that large molecules were degraded at 250 °C. This indicated that pretreatment with FeCl₃ and a high temperature caused more small molecules to form. Pretreatment near the critical point of methanol strongly decreased the M_w of the MSFe and MAFe products.

3.2.2. GC-MS analysis of the liquid products

The compounds in the liquid products were identified by GC-MS. At 225 °C, more detectable products were formed from MSFe than MAFe. It can be seen from Fig. 5(a) that the largest peak was for 2-propenoic acid, 3-(4-hydroxyphenyl)-, methyl ester (peak 9), which contributed 21.66% of the total area of the 14 largest peaks (excluding the peak for 2,6-di-*tert*-butyl-4-methylphenol (BHT)). The second-largest peak was for 2-furanethanol, beta-methoxy-(S)- (peak 1), a furfural derivative, which contributed 14.79% of the total area of the 14 largest peaks. The next largest peak was for beta-D-arabinopyranoside, methyl (peak 6), which contributed 14.32% of the total area of the 14 largest peaks.

At 225 °C, the main liquid products of MSFe were furfural derivatives, esters, carbohydrate derivatives, and macromolecular phenol derivatives. The main products of MAFe were similar to the main products of MSFe except that much smaller amounts of furfural derivatives were produced. The main products of DM were phenol derivatives. This indicated that FeCl₃ and *Miscanthus* strongly interacted during the pre-soaking process. The furfural derivatives, carbohydrate derivatives, and macromolecular phenol derivatives might have been produced from cellulose, hemicellulose, and lignin, respectively. The esters might have been produced through the opening of phenol rings.

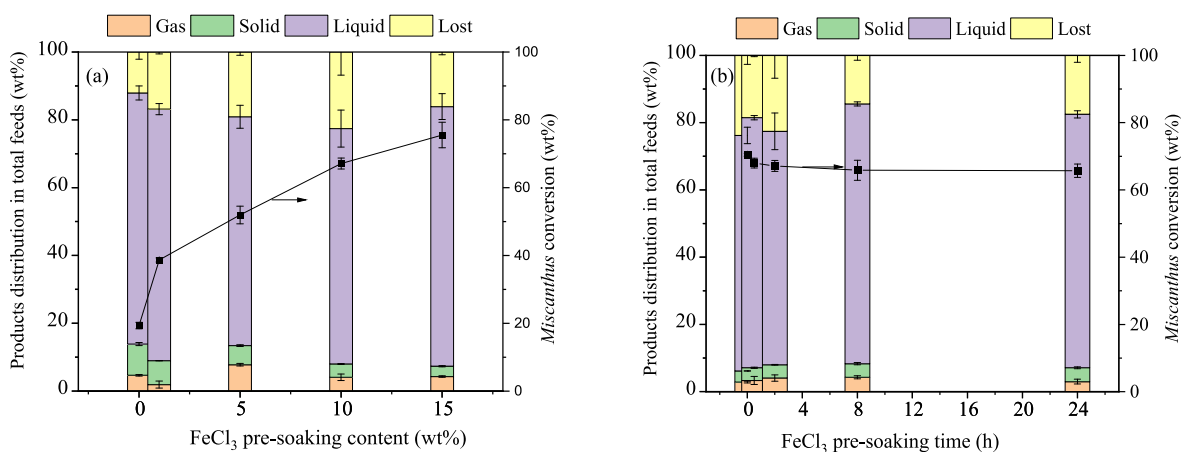


Fig. 3. Product distributions and conversion rates for *Miscanthus* reacted (a) at 250 °C with different FeCl₃ pre-soaking contents and (b) at 250 °C with different FeCl₃ pre-soaking times.

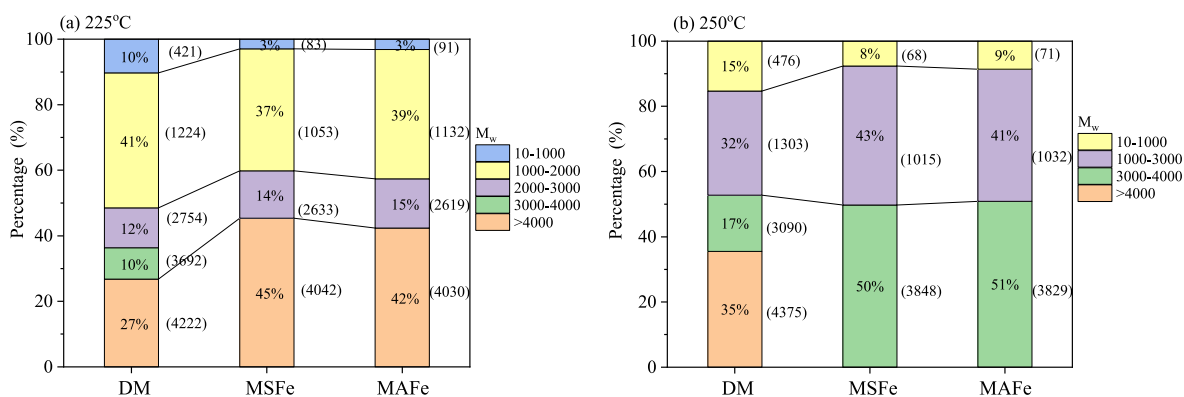


Fig. 4. Molecular weight distributions of the liquid products of the reactions performed at (a) 225 °C and (b) 250 °C.

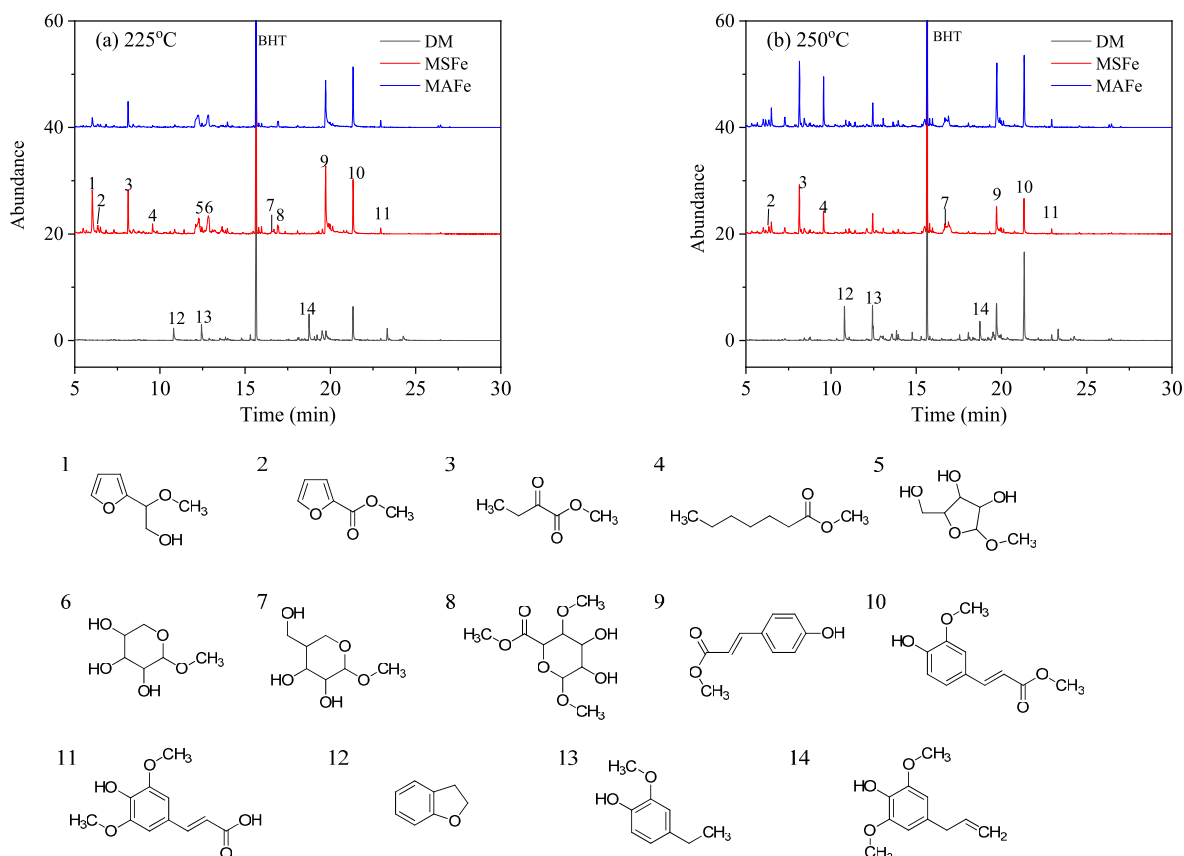


Fig. 5. Gas chromatography mass spectrometry results for the liquid products of the reactions performed at (a) 225 °C and (b) 250 °C.

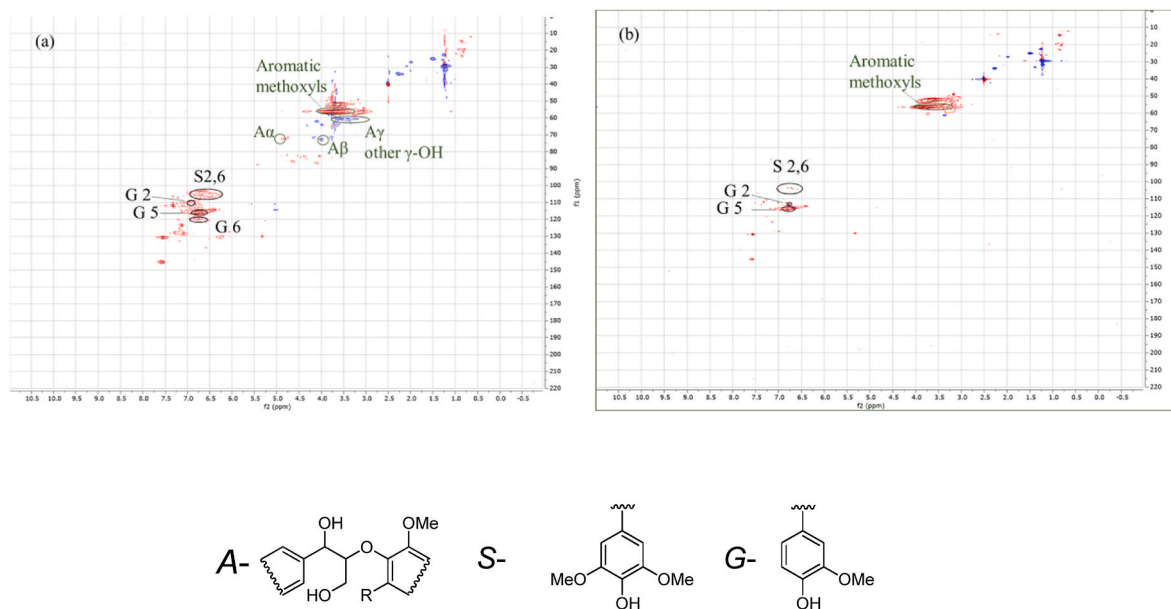
FeCl₃ therefore facilitated degradation of both the feedstocks and intermediates.

The chemicals in the products of MSFe and MAFe were similar when the reaction temperature was 250 °C, as shown in Fig. 5(b). Furfural and carbohydrate derivatives contributed slightly less to the MSFe products than the MAFe products, indicating that the furfural and carbohydrate derivatives were not stable at high temperatures. This might have been because FeCl₃ promoted degradation of the furfural and carbohydrate derivatives and the formation of new small molecules. More chemicals were present in the DM products at higher than lower temperatures, which would mainly have been caused by more degradation of *Miscanthus* occurring as the temperature increased. Pre-soaking in FeCl₃ was found to be conducive to the degradation of cellulose and

hemicellulose and to cause larger amounts of furfural and carbohydrate derivatives to form. Pre-soaking in FeCl₃ can allow a lower reaction temperature to be used when liquefying biomass.

3.2.3. HSQC spectra of the liquid products

The HSQC spectra of the liquid products of DM and MSFe reacted at 250 °C are shown in Fig. 6. It can be seen from Fig. 6(a) that the DM products contained many lignin (β -O-4') fragments (A-), and it can be seen from Fig. 6(b) that A α , A β , and A γ structures were found at very low abundances in the liquid products of MSFe. This indicated that FeCl₃ assisted in breaking the β -O-4' bonds in the A- fragments. FeCl₃ could break β -O-4' bonds by chelating with the phenolic groups [29,30]. Smaller amounts of syringyl and guaiacyl were found in the MSFe



S- and G- are syringol and guaiacol units, respectively.

Fig. 6. Heteronuclear single quantum coherence spectra of the liquid products of (a) dried *Miscanthus* and (b) *Miscanthus* pre-soaked in FeCl_3 reacted at 250 °C.

products than the DM products, indicating that FeCl_3 also facilitated the degradation of lignin.

3.2.4. Fe contents of the liquid products

The Fe distribution was assessed by determining the Fe contents of the liquid products. As shown in Fig. 7, the Fe contents of the liquid products of MSFe and MAFe decreased markedly as the temperature increased. When the reaction temperature was 150 °C, the Fe contents of the liquid products of MSFe and MAFe were 21.74 and 26.50 mg, respectively, corresponding to 63.21% and 77.05%, respectively, of the total amount of Fe added. When the reaction temperature was 350 °C, the Fe contents of the liquid products of MSFe and MAFe were 2.75 and 4.63 mg, respectively, corresponding to 7.98% and 13.46%, respectively, of the total amount of Fe added. It was found in previous studies that increasing the reaction temperature caused larger amounts of

metals in biomass to enter the solid products [31,32].

The Fe contents were lower for the liquid products of MSFe than the liquid products of MAFe at all of the reaction temperatures, indicating that more Fe was retained in the MSFe solid products than the MAFe solid products. This would mean it will be easier to recover the Fe catalyst (e.g., through incineration) from MSFe than MAFe. Fe entered the MAFe and MSFe solid products more quickly as the reaction temperature increased. This may have been because the Fe in MSFe became homogeneously distributed in the reactor when supercritical methanol was present and then Fe formed Fe_3O_4 in the solid products. Pre-soaking in FeCl_3 therefore had a stronger effect at lower temperatures than higher temperatures.

3.3. Characterization of the raw materials and solid products

3.3.1. TGA of the raw materials

Decomposition of DM and MSFe in the temperature range 0–800 °C was investigated by TGA. Differential thermogravimetry curves for DM and MSFe are shown in Fig. 8. MSFe decomposed over a broader temperature range than DM, and the temperatures at which maximum decomposition occurred for DM and MSFe were 365 and 345 °C, respectively, indicating that MSFe decomposed at a lower temperature than DM, i.e., adding Fe caused *Miscanthus* to decompose at a lower temperature. The maximum reaction rate for MSFe was 7.9% min^{-1} , which was slightly lower than the maximum reaction rate for DM (10.5% min^{-1}). This was consistent with the results of a study performed by Zeng et al. in which Fe^{3+} was found to hinder the thermal decomposition of lignin [26]. This may have been caused by Fe remaining in the MSFe residue at high temperatures, causing the decomposition rate to be lower than if Fe was not present.

3.3.2. FTIR spectroscopy of DM and the solid products

The FTIR spectra of the DM and the solid products were acquired to attempt to identify the products and the reactions that occurred. The spectra are shown in Fig. 9. The FTIR spectra for each sample contained an obvious hydroxyl and carboxyl group O–H stretching peak at a wavenumber of 3426 cm^{-1} , which was very similar in the DM and solid product spectra. A peak at 2848 cm^{-1} in the DM spectrum was not

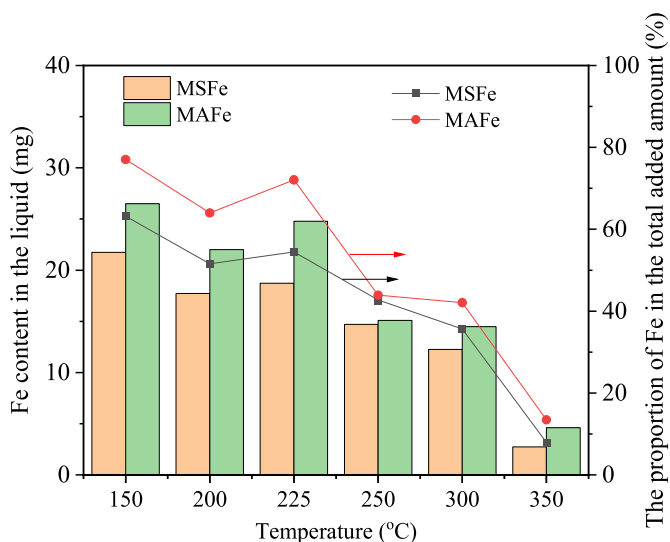


Fig. 7. Fe contents of the liquid products of the reactions at different temperatures.

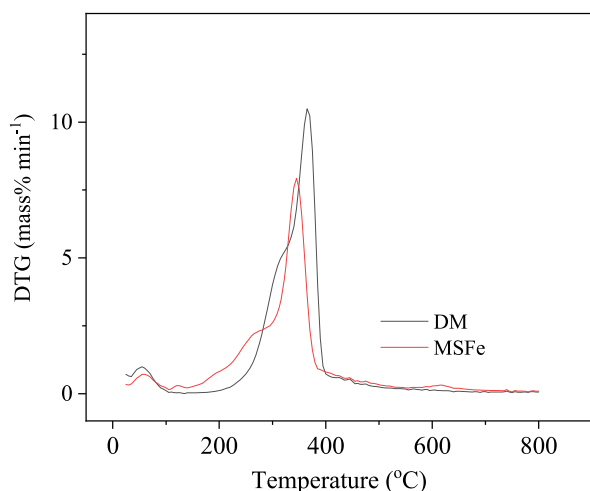


Fig. 8. Differential thermogravimetry curves for dried *Miscanthus* (DM) and *Miscanthus* pre-soaked in FeCl_3 (MSFe).

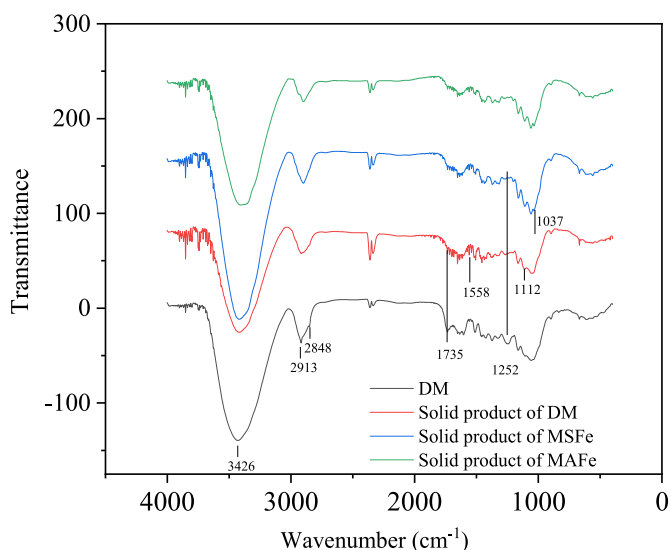


Fig. 9. Fourier-transform infrared spectra for dried *Miscanthus* (DM) and the solid products of DM, *Miscanthus* pre-soaked in FeCl_3 (MSFe), and *Miscanthus* with FeCl_3 added directly (MAFe) at a reaction temperature of 250 °C.

present in the product spectra, indicating that the reactions removed alkyl groups. Peaks for double bonds in the range 1735–1558 cm^{-1} were present in the solid product spectra, indicating that the reactions increased the numbers of C=O bonds (indicated by the peaks at 1720, 1700, and 1683 cm^{-1}) and/or C=C bonds (indicated by the peak at 1652 cm^{-1}). This may have been caused by oxidization of O–H bonds to give C=O bonds and some aromatization of the solid products.

The peak at 1252 cm^{-1} was smaller in the spectra for the solid products of DM, MSFe, and MAFe than in the spectrum for raw DM, indicating that the reactions caused some C–O bonds in lignin to break. The 1252 cm^{-1} peak was much smaller in the MSFe and MAFe product spectra than the other spectra, indicating that adding FeCl_3 caused more C–O bonds to break. This was consistent with the HSQC results (Fig. 6), which indicated that β -O-4' bonds disappeared during the reactions. The reactions caused alcohol C–O peaks to appear at 1112 cm^{-1} in the DM solid product spectrum and 1037 cm^{-1} in the MSFe and MAFe solid product spectra. This may have been caused by alcohols being produced because methanol reacted and combined with the solid. These results indicated that Fe can cause β -O-4' bonds to break and more reactions between methanol and *Miscanthus* to occur.

3.3.3. X-ray diffractometry of the solid products

The X-ray diffractometry patterns of the solid products of MSFe and MAFe at different reaction temperatures are shown in Fig. 10. Some cellulose and turbostratic carbon were found in the solid products from reaction temperatures of 150 and 250 °C [33]. When the reaction temperature was 150 °C, there was more turbostratic carbon in the MSFe product than the MAFe product, indicating that Fe interacted more with the *Miscanthus* at low temperatures when the *Miscanthus* was pre-soaked in FeCl_3 than when FeCl_3 was added directly. This also confirmed that pre-soaking in Fe had more effect when the reaction temperature was lower than when the reaction temperature was higher. When the reaction temperature was 350 °C, Fe_3O_4 was present in the solid products of both MSFe and MAFe. This may have been because phenolic compounds were generated during the reactions. Phenolic compounds are reducing agents and could cause Fe_3O_4 to form [34].

4. Discussion

4.1. Expected pathways for the formation of the main products

It can be seen from the GC-MS results shown in Fig. 5 that phenol derivatives, furfural derivatives, and carbohydrate derivatives were the most common liquid products. Phenol derivatives could be generated from lignin units [35–39], furfural derivatives could be generated from cellulose, hemicellulose, or intermediate cellulose and hemicellulose degradation compounds [40,41], and carbohydrate derivatives could be generated from cellulose [41], as shown in Fig. 11.

Phenol derivatives could form through an alcohol group (–OH) in lignin fragments becoming oxidized to give a carboxylic acid group and then the carboxylic acid group reacting with methanol to give the corresponding ester group. Güvenatam et al. [42] found that ethanol was involved in alkylation reactions when soda lignin was depolymerized in a supercritical mixture of ethanol and water. Furfural derivatives could form through the dehydration of sugars, and carbohydrate derivatives could form through the hydrolysis of cellulose.

4.2. Role of Fe in MSFe

It can be seen from Figs. 1 and 8 that FeCl_3 strongly improved the *Miscanthus* conversion process. FeCl_3 strongly increased the amount of degradation of large molecules that occurred, as shown in Figs. 4 and 9), caused more chemicals to be formed (Fig. 5), and caused β -O-4' bonds to break and therefore more fragments to form. These reactions were attributed to Fe^{3+} increasing the amounts of the reactions that occurred by forming chelates with phenolic groups [29,30]. As shown in Fig. 7, the Fe content was higher for the MAFe liquid products than the MSFe

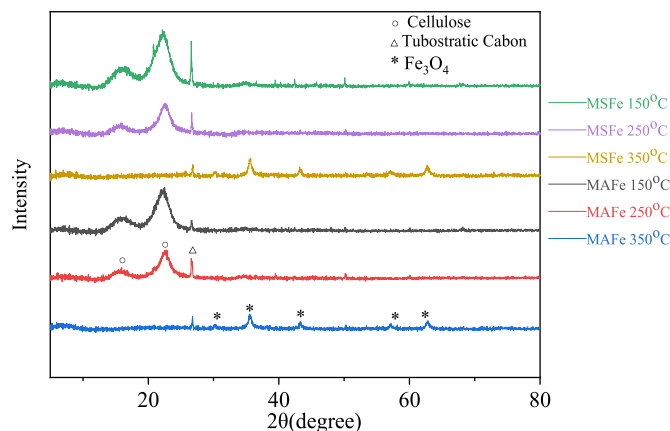


Fig. 10. X-ray diffractometry patterns of the solid products of *Miscanthus* pre-soaked in FeCl_3 (MSFe) and *Miscanthus* with FeCl_3 added directly (MAFe) at different reaction temperatures.

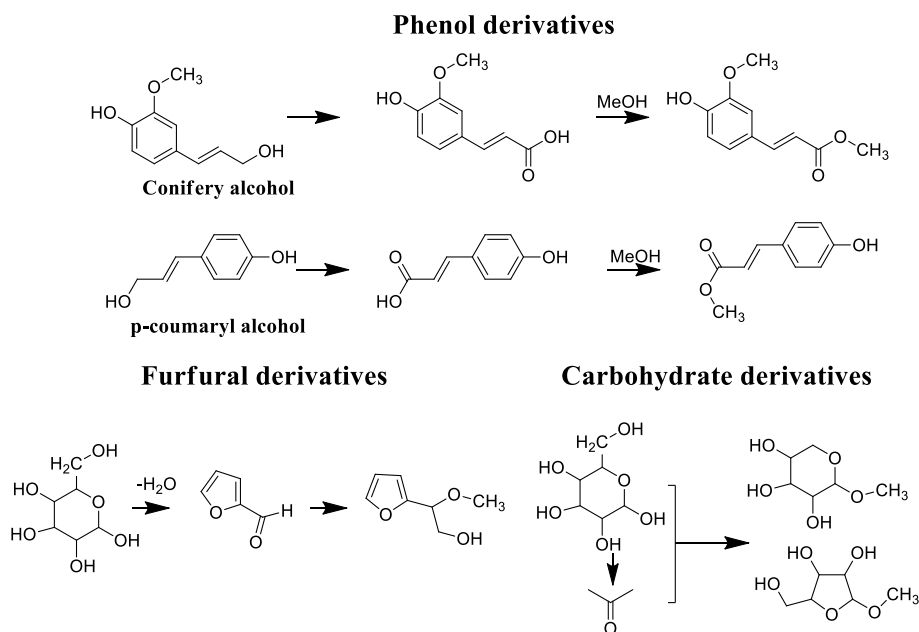


Fig. 11. Expected pathways through which the main chemicals formed.

liquid products, indicating that more Fe remained in the MSFe solid products than the MAFe solid products and that Fe became attached to the *Miscanthus* during the pre-soaking process. Pre-soaking therefore contributed to the increases in the *Miscanthus* conversion rate and amounts of high-value-added chemicals produced and caused the solid products to contain more Fe^{3+} .

The expected roles of pre-soaking with FeCl_3 in *Miscanthus* liquefaction are shown in Fig. 12. During the reactions at temperatures $<225\text{ }^\circ\text{C}$, methanol will be subcritical. The Fe concentration in the microenvironment near the *Miscanthus* will therefore be higher for MSFe than MAFe, and a concentration gradient will form, meaning more phenols and furfural derivatives will be produced from MSFe than MAFe. At reaction temperatures $>250\text{ }^\circ\text{C}$ methanol will be a supercritical fluid, so the Fe will mix completely with the *Miscanthus* whether the *Miscanthus* has been soaked with Fe or the Fe has been added to the reaction vessel. The compounds produced from MAFe and MSFe and the concentrations of the compounds will be similar at reaction temperatures $>250\text{ }^\circ\text{C}$, and there will be no clear advantage of pre-soaking the *Miscanthus*. Pre-soaking the *Miscanthus* in FeCl_3 to catalyze the reaction is therefore beneficial only at low temperatures ($<250\text{ }^\circ\text{C}$).

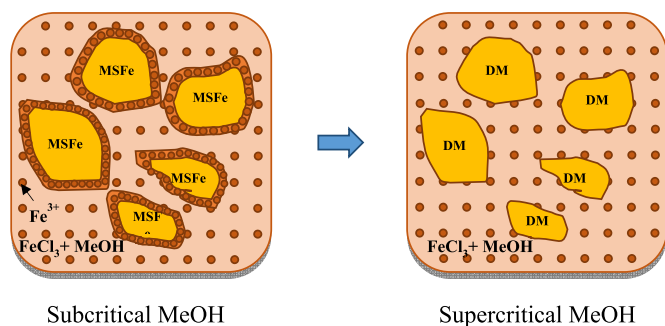


Fig. 12. Expected roles of pre-soaking with FeCl_3 in *Miscanthus* liquefaction with subcritical and supercritical MeOH.

4.3. Limitations and solutions

The study was limited because many chemical derivatives such as phenol derivatives and furfural derivatives were obtained, possibly because methanol was used as the solvent. It can be seen from Fig. 11 that phenols formed first, then the phenols reacted with methanol to give phenol derivatives. It would therefore be better to use a milder solvent (e.g., a mixture of methanol and water) to prevent the phenols taking part in reactions. Another possibility would be to add catalysts to aid the conversion of the derivatives into value-added chemicals.

In future applications of the method, environmental sustainability should be considered carefully [43]. The whole process should be analyzed from the thermodynamic, economic, and environmental points of view using exergy-based methods and particularly exergy-based environmental methods [44].

5. Conclusions and prospects

Pre-soaking *Miscanthus* in FeCl_3 before liquefaction in subcritical methanol can give a higher conversion rate and more value-added chemical derivatives than can be given by adding the FeCl_3 directly to the liquefaction reactor. Pre-soaking is particularly useful to ensure that the catalyst is homogeneously distributed in a continuous reactor, to decrease corrosion of the reactor. Much more research is required to identify the most appropriate solvents and catalysts to prevent derivatives forming and improve the value-added-chemical yields. The main conclusions are summarized below.

- (1) Increasing the temperature caused the MSFe and MAFe conversion rates to increase more than the DM conversion rate, but this effect was not found when the temperature reached $350\text{ }^\circ\text{C}$, possibly because of re-polymerization of intermediate products and formation of Fe_3O_4 . Increasing the FeCl_3 concentration caused the *Miscanthus* conversion rate to increase. The soaking time has little effect on the *Miscanthus* conversion rate.
- (2) At $225\text{ }^\circ\text{C}$, the MSFe and MAFe conversion rates were 45.1% and 36.1%, respectively, but at $250\text{ }^\circ\text{C}$, the MSFe and MAFe conversion rates were 67.1% and 70.4%, respectively. At both temperatures, more phenol derivatives, furfural derivatives,

carbohydrate derivatives, and esters were produced during the solvothermal liquefaction of MSFe and MAFe in methanol than during the solvothermal liquefaction of DM in methanol. More furfural derivatives were produced from MSFe than MAFe and DM at low temperatures.

- (3) More Fe was retained in the solid products of MSFe than MAFe. The Fe content of the liquid product was lower for MSFe than MAFe at all reaction temperatures. Increasing the reaction temperature caused the Fe in the liquid products of MAFe and MSFe to enter the solid quickly.
- (4) Subcritical conditions were more suitable for MSFe liquefaction than MAFe and DM liquefaction because the Fe in MSFe helped break ether bonds and was at a higher concentration in the microenvironment near the *Miscanthus* material in MSFe than MAFe and therefore more effectively promoted decomposition of the *Miscanthus* in MSFe than MAFe.

Credit author statement

Ying Su: Conceptualization, Methodology, Resources, Data Curation, Formal analysis, Visualization, Writing - Original Draft; Bingfeng Guo: Methodology, Resources, Writing - Review & Editing, Ursel Hornung: Funding acquisition, Writing - Review & Editing, Nicolaus Dahmen: Funding acquisition, Writing - Review & Editing.

Declaration of competing interest

The authors declare that they have no known competing financial interests or personal relationships that could have appeared to influence the work reported in this paper.

Data availability

Data will be made available on request.

Acknowledgments

The authors gratefully acknowledge financial support from the China Scholarship Council. The authors gratefully acknowledge the support from the Ministry of Housing and Urban-Rural Development of the People's Republic of China research and development project (2016-K4-031). The authors thank Armin Lautenbach, Birgit Rolli, Veronika Holdried, Yannick Trautlein, and Marion Lenzner for skillful technical assistance. The authors thank Thomas Tietz and Matthias Pagel for mechanical support. The authors thank Klaus Raffelt, Maximilian Worner, and Joscha Zimmermann for their constructive suggestions. We thank Gareth Thomas, PhD, from Liwen Bianji (Edanz) (<https://www.liwenbianji.cn>), for editing the language of a draft of this manuscript.

References

- [1] Tursi A. A review on biomass: importance, chemistry, classification, and conversion. *Biofuel Res J* 2019;6(2):962–79.
- [2] Brosse N, Dufour A, Meng X, Sun Q, Ragauskas A. *Miscanthus*: a fast-growing crop for biofuels and chemicals production. *Biofuels, Bioprod Biorefin* 2012;6(5):580–98.
- [3] Dahmen N, Lewandowski I, Zibek S, Weidmann A. Integrated lignocellulosic value chains in a growing bioeconomy: status quo and perspectives. *GCB Bioenergy* 2019;11(1):107–17.
- [4] Wang F, Yu YZ, Chen Y, Yang CY, Yang YY. One-step alcoholysis of lignin into small-molecular aromatics: influence of temperature, solvent, and catalyst. *Biotechnol Rep* 2019;24:e00363–71.
- [5] Wu Z, Zhao X, Zhang J, Li X, Zhang Y, Wang F. Ethanol/1,4-dioxane/formic acid as synergistic solvents for the conversion of lignin into high-value added phenolic monomers. *Bioresour Technol* 2019;278:187–94.
- [6] Lee CBT, Wu TY. A review on solvent systems for furfural production from lignocellulosic biomass. *Renew Sustain Energy Rev* 2021:137.
- [7] Beims RF, Hu YL, Shui HF, Xu CB. Hydrothermal liquefaction of biomass to fuels and value-added chemicals: products applications and challenges to develop large-scale operations. *Biomass Bioenergy* 2020;135:105510–23.
- [8] Toor SS, Rosendahl L, Rudolf A. Hydrothermal liquefaction of biomass: a review of subcritical water technologies. *Energy* 2011;36(5):2328–42.
- [9] Lu J, Liu Z, Zhang Y, Savage PE. 110th anniversary: influence of solvents on biocrude from hydrothermal liquefaction of soybean oil, soy protein, cellulose, xylose, and lignin, and their quinary mixture. *Ind Eng Chem Res* 2019;58(31):13971–6.
- [10] Huang HJ, Yuan XZ. Recent progress in the direct liquefaction of typical biomass. *Prog Energy Combust Sci* 2015;49:59–80.
- [11] Zhai QL, Li FL, Wang F, Xu JM, Jiang JC, Cai ZS. Liquefaction of poplar biomass for value-added platform chemicals. *Cellulose* 2018;25(8):4663–75.
- [12] Nonchana T, Piantong K. Bio-oil synthesis from cassava pulp via hydrothermal liquefaction: effects of catalysts and operating conditions. *Int J Renew Energy Dev* 2020;9(3):329–36.
- [13] Hongbo D, Deng F, Kommalapati RR, Amarasekara AS. Iron based catalysts in biomass processing. *Renew Sustain Energy Rev* 2020;134:110292–306.
- [14] de Caprariis B, Bavasso I, Bracciale MP, Damizia M, De Filippis P, Scarsella M. Enhanced bio-crude yield and quality by reductive hydrothermal liquefaction of oak wood biomass: effect of iron addition. *J Anal Appl Pyrolysis* 2019;139:123–30.
- [15] Chen YW, Lee HV. Recent progress in homogeneous Lewis acid catalysts for the transformation of hemicellulose and cellulose into valuable chemicals, fuels, and nanocellulose. *Rev Chem Eng* 2020;36(2):215–35.
- [16] Ding D, Hu J, Hui L, Liu Z, Shao L. Valorization of *Miscanthus × giganteus* by γ -Valerolactone/H₂O/FeCl₃ system toward efficient conversion of cellulose and hemicelluloses. *Carbohydr Polym* 2021;270:118388–97.
- [17] Kang KE, Park DH, Jeong GT. Effects of inorganic salts on pretreatment of *Miscanthus* straw. *Bioresour Technol* 2013;132:160–5.
- [18] Chen L, Chen R, Fu S. Preliminary exploration on pretreatment with metal chlorides and enzymatic hydrolysis of bagasse. *Biomass Bioenergy* 2014;71:311–7.
- [19] Chen Y, Zhou Y, Zhang R, Hu C. Conversion of saccharides in enteromorpha prolifera to furfurals in the presence of FeCl₃. *Mol Catal* 2020;484:110729–36.
- [20] Amarasekara AS, Deng F. Single reagent treatment and degradation of switchgrass using iron(III)chloride: the effects on hemicellulose, cellulose and lignin. *Biomass Bioenergy* 2019;131:105421–7.
- [21] Zhao B, Hu Y, Qi L, Gao J, Zhao G, Ray MB, Xu CC. Promotion effects of metallic iron on hydrothermal liquefaction of cornstalk in ethanol-water mixed solvents for the production of biocrude oil. *Fuel* 2021;285:119150–9.
- [22] Patil V, Adhikari S, Cross P, Jahromi H. Progress in the solvent depolymerization of lignin. *Renew Sustain Energy Rev* 2020;133:110359–78.
- [23] Zeb H, Choi J, Kim Y, Kim J. A new role of supercritical ethanol in macroalgae liquefaction (*Saccharina japonica*): understanding ethanol participation, yield, and energy efficiency. *Energy* 2017;118:116–26.
- [24] Yan B, Lin X, Chen Z, Cai Q, Zhang S. Selective production of phenolic monomers via high efficient lignin depolymerization with a carbon based nickel-iron-molybdenum carbide catalyst under mild conditions. *Bioresour Technol* 2021;321:124503–10.
- [25] Kumaniaev I, Subbotina E, Savmarker J, Larhed M, Galkin MV, Samec JSM. Lignin depolymerization to monophenolic compounds in a flow-through system. *Green Chem* 2017;19(24):5767–71.
- [26] Zeng J, Yoo CG, Wang F, Pan X, Vermerris W, Tong Z. Biomimetic Fenton-catalyzed lignin depolymerization to high-value aromatics and dicarboxylic acids. *ChemSusChem* 2015;8(5):861–71.
- [27] Poling BE, Prausnitz JM, O'Connell JP. The properties of gases and liquids. fifth ed. McGraw Hill; 2000.
- [28] Perera SM, Wickramasinghe C, Samarasinghe B, Narayana M. Modeling of thermochemical conversion of waste biomass—a comprehensive review. *Biofuel Res J* 2021;8(4):1481–528.
- [29] Khokhar S, Owusu Apenten RK. Iron binding characteristics of phenolic compounds: some tentative structure-activity relations. *Food Chem* 2003;81(1):133–40.
- [30] Pangkumhang B, Phanthasri J, Suwannatnai S, Khamdahsag P, Lin C, Tanboonchuy V. Optimization of lignin removal from synthesized wastewater by iron (III) trimesate. *Environment and Natural Resources Journal* 2019;17(4):1–10.
- [31] Xu Z, Zhu W, Bao J, Chen J. The fate of heavy metal during subcritical and supercritical water gasification of sewage sludge. In: International symposium on water resource and environmental protection. IEEE 2011; 2011. p. 1260–3.
- [32] Yuan X, Huang H, Zeng G, Li H, Wang J, Zhou C, Zhu H, Pei X, Liu Z, Liu Z. Total concentrations and chemical speciation of heavy metals in liquefaction residues of sewage sludge. *Bioresour Technol* 2011;102(5):4104–10.
- [33] Li H, Hurley S, Xu C. Liquefactions of peat in supercritical water with a novel iron catalyst. *Fuel* 2011;90(1):412–20.
- [34] Bouafia A, Laouini SE, Khelef A, Tedjani ML, Guemari F. Effect of ferric chloride concentration on the type of magnetite (Fe₃O₄) nanoparticles biosynthesized by aqueous leaves extract of artemisia and assessment of their antioxidant activities. *J Cluster Sci* 2020;32(4):1033–41.
- [35] Forchheim D, Hornung U, Kruse A, Sutter T. Kinetic modelling of hydrothermal lignin depolymerisation. *Waste Biomass Valorization* 2014;5(6):985–94.
- [36] Schuler J, Hornung U, Kruse A, Dahmen N, Sauer J. Hydrothermal liquefaction of lignin. *J Biomaterials Nanobiotechnology* 2017;8:96–108. 01.
- [37] Breunig M, Gebhart P, Hornung U, Kruse A, Dinjus E. Direct liquefaction of lignin and lignin rich biomasses by heterogenic catalytic hydrogenolysis. *Biomass Bioenergy* 2018;111:352–60.
- [38] Gasson JR, Forchheim D, Sutter T, Hornung U, Kruse A, Barth T. Modeling the lignin degradation kinetics in an ethanol/formic acid solvolysis approach. Part 1. Kinetic model development. *Ind Eng Chem Res* 2012;51(32):10595–606.
- [39] Forchheim D, Gasson JR, Hornung U, Kruse A, Barth T. Modeling the lignin degradation kinetics in an ethanol/formic acid solvolysis approach. Part 2.

- Validation and transfer to variable conditions. *Ind Eng Chem Res* 2012;51(46): 15053–63.
- [40] Schwiderski M, Kruse A, Grandl R, Dockendorf D. Kinetics of the AlCl₃ catalyzed xylan hydrolysis during Methanosolv pulping of beech wood. *RSC Adv* 2014;4(85): 45118–27.
- [41] Kruse A, Maniam P, Spieler F. Influence of proteins on the hydrothermal gasification and liquefaction of biomass. 2. Model compounds. *Ind Eng Chem Res* 2007;46(1):87–96.
- [42] Güvenatam B, Heeres EHJ, Pidko EA, Hensen EJM. Lewis acid-catalyzed depolymerization of soda lignin in supercritical ethanol/water mixtures. *Catal Today* 2016;269:9–20.
- [43] Rosen MA. Environmental sustainability tools in the biofuel industry. *Biofuel Res J* 2018;5(1):751–2.
- [44] Aghbashlo M, Khounani Z, Hosseinzadeh-Bandbafha H, Gupta VK, Amiri H, Lam SS, Morosuk T, Tabatabaei M. Exergoenvironmental analysis of bioenergy systems: a comprehensive review. *Renew Sustain Energy Rev* 2021;149: 111399–418.